AIP | Review of Scientific Instruments

Monitoring plasma treatment of thin films by surface plasmon resonance

Ranjit Laha, A. Manivannan, and S. Kasiviswanathan

Citation: Review of Scientific Instruments **85**, 035001 (2014); doi: 10.1063/1.4866241
View online: http://dx.doi.org/10.1063/1.4866241
View Table of Contents: http://scitation.aip.org/content/aip/journal/rsi/85/3?ver=pdfcov
Published by the AIP Publishing

Monitoring plasma treatment of thin films by surface plasmon resonance

Ranjit Laha,[1,a)] A. Manivannan,[2] and S. Kasiviswanathan[3]
[1]*Department of Physics, National Institute of Technology Raipur, 492010 Raipur, India*
[2]*US Department of Energy, National Energy Technology Laboratory, Morgantown, West Virginia 26507, USA*
[3]*Department of Physics, Indian Institute of Technology Madras, 600036 Chennai, India*

(Received 31 December 2013; accepted 6 February 2014; published online 3 March 2014)

We report the surface plasmon resonance (SPR) measurements during plasma treatment of thin films by an indigenously designed setup. From the measurements on Al (6.3 nm)/Ag (38 nm) bi-layer at a pressure of 0.02 mbar, the SPR position was found to be shifted by ∼20° after a plasma treatment of ∼7 h. The formation of oxide layers during plasma oxidation was confirmed by glancing angle x-ray diffraction (GXRD) measurements. Combined analysis of GXRD and SPR data confirmed that while top Al layer enables controlling plasma oxidation of Ag, the setup enables monitoring the same. The setup designed is a first of its kind for *in situ* SPR studies where creation of low pressure is a prerequisite. © *2014 AIP Publishing LLC*. [http://dx.doi.org/10.1063/1.4866241]

I. INTRODUCTION

Photon-coupled quantum of electron excitation at a metal-dielectric interface is called surface plasmon. Surface plasmon resonance (SPR) is the process of absorption of incident light by surface plasmons under optimum condition.[1,2] The said optimum condition arises when the interface-parallel component of the wave vector of the incident light matches with the wave vector ($\mathbf{k}_{SP}$) of the plasmon wave moving along the interface. The dispersion relation for the surface plasmons at a metal–dielectric interface is given as[2]

$$k_{SP} = \frac{\omega}{c}\sqrt{\frac{\varepsilon_m \varepsilon_d}{\varepsilon_m + \varepsilon_d}}, \quad (1)$$

where ω is the angular frequency of the incident radiation, and ε_m and ε_d are the dielectric function of the metal and dielectric constant of the dielectric medium, respectively. For most of the metals, the real part of the dielectric function has a large negative value for frequencies in the visible spectrum, and the magnitude of $\mathbf{k}_{SP}$ is greater than that of the incident light at the same frequency. Therefore, suitable couplers are required in order to generate the resonant surface plasmons. Usually, attenuated total reflection (ATR) technique[2] is used to match the wave vector of the incident light to that of the surface plasmons. In the widely used Kretschmann configuration, a beam of p-polarized light is made to fall on a prism coated with a metal of suitable thickness and the intensity of the reflected light is detected as a function of the angle of incidence. At a particular angle of incidence, the resonance condition is satisfied and a sharp fall in the reflectivity is observed as the signature of resonance.

SPR phenomenon is extremely sensitive to the changes in the refractive index and the thickness of the dielectric medium adjacent to the metal layer. Hence, any change to the metal thin film or to the medium near to it can easily be detected by SPR technique thereby making SPR as one of the most sought sensing tools.[3,4] Most of the SPR based sensors mainly detect the concentration and kinetics of adsorbed molecules, in atmospheric conditions. However, there are certain processes which need creation of low pressure as a prerequisite. Plasma treatment of thin films, for example, is one of such processes. Recently, plasma treatment has been found to be extremely useful in research on nanoscience.[5,6] Though use of SPR to study the oxidation is not new, the present work of SPR measurements during plasma oxidation is a first one of its kind for the following reasons. Yang *et al.*[7] have used SPR technique to study the natural (atmospheric) oxidation of Al. Park *et al.*[8] and Knechten[9] have used SPR to study plasma oxidation of Al film. In none of the earlier works, however, SPR studies during plasma treatment have been done. In order to perform such studies, there should be provision for SPR measurements without vacuum break. In the present work, we report the design and fabrication of a setup that is capable of performing SPR measurements during plasma treatment. The setup is based on excitation of surface plasmons, with prism based Kretschmann configuration in angle interrogation mode, inside a vacuum chamber with or without the presence of plasma. SPR measurements during plasma treatment of Al\Ag bi-layer are reported to vindicate the usefulness of the setup.

II. EXPERIMENTAL DETAILS

Figure 1 shows the schematic of the setup developed for SPR under vacuum. The setup and the experiments therewith have four major parts such as arrangement for SPR detection inside a vacuum chamber, a pumping station to achieve the required low pressure, the arrangement including separate power source to obtain plasma, and interfacing required for SPR measurements with and without plasma.

The first part of the design makes use of the two-prism setup[10] for SPR measurements. The advantage of the two-prism setup is to record SPR data for larger angular range in one stretch using a single photo detector. In the setup, a p-polarized beam of He-Ne laser with output at 632.8 nm was used to excite plasmons. A rotational stage, driven by a stepper motor with a step size of 0.02°, provides relative

a)Author to whom correspondence should be addressed. Electronic mail: laharanjit@gmail.com

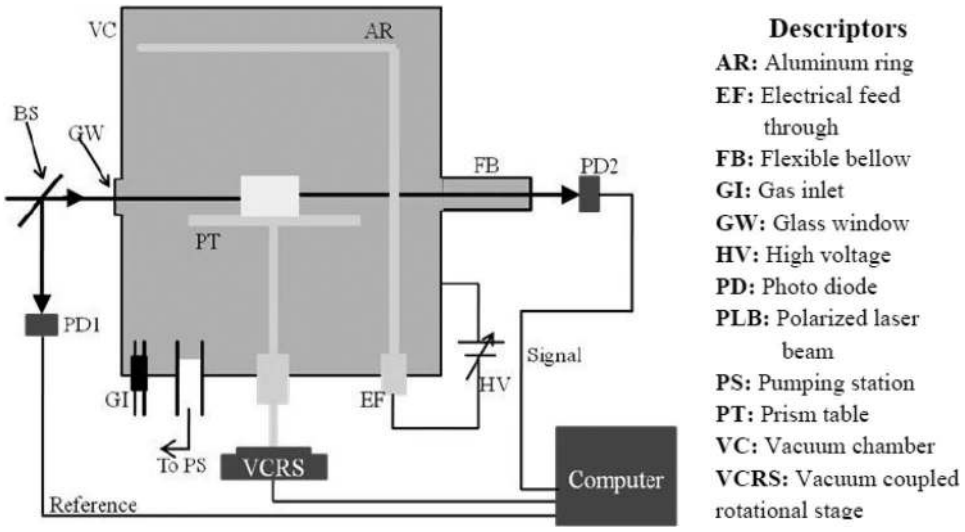

FIG. 1. Schematic of the setup developed for SPR under vacuum.

movement of the prisms with respect to the incident laser beam. In order to facilitate the motion of prism inside the vacuum chamber with the controlling being done outside, the rotational stage was coupled suitably into the chamber. After each step of rotation of the prisms, the intensities of the reference and the emergent beams were measured by identical photodiodes using a simultaneous sampling data acquisition card. The relative intensity was calculated as the ratio of the reflected signal to the reference signal. Signal handling and stepper motor motion control were done through an interfaced computer. In order to make SPR studies during plasma oxidation, a dc glow discharge arrangement was added inside the vacuum chamber. The geometry used in the arrangement consists of a circular Al ring as cathode producing uniform glow of plasma. The glow obtained with such a geometry does not contain the structures such as Faraday dark space and positive column usually observed in cylindrical plasmas.[11] Gas inlet to the chamber was arranged in such a way that different gas sources (e.g., gas cylinders) can be connected externally as and when required. The Al ring was fixed inside the chamber in such a way that the prisms containing samples could be directly exposed to plasma during SPR measurements. More importantly, since the prism table is fully immersed in the plasma glow, no multiple reflections created due to plasma intensity can have interference with the ATR signal received by photodiode from the prisms. The setup also facilitates SPR measurements during plasma treatment without disturbing the detector positions. Thus, the design negates the effect of angular position of detector on the SPR intensities.[12]

For experiments involving plasma, the plasma was created by using a dc supply of 400 V at 0.05 mbar which was reached by inletting oxygen gas from a base pressure of 0.02 mbar. The way of SPR measurement with a two-prism setup is shown in Fig. 2. Figure 2(a) shows the top view of the two prisms shown in Fig. 1 along with the ray diagram, whereas Fig. 2(b) shows the typical SPR spectrum obtained with a two-prism setup. The face BC in Fig. 2(a) is seen in the front view of Fig. 1 with the axis of rotation of prism table passing through the midpoint of AB and normal to the plane ABC. The films under study were coated by thermal evaporation at a chamber pressure of $\sim 10^{-6}$ mbar onto the hypotenuse face BC of the first prism as shown in Fig. 2(a). Though the relative intensity of the emergent beam is usually plotted against the angle θ at the metal-prism interface as shown in Fig. 2(a) for the purpose of theoretical calculations, it can also be plotted against α, as only α is accessible during experiments with the present design. Hence, the spectrum shown in Fig. 2(b) as well as the spectra presented in this paper hereafter are all plotted as a function of α. The relation between the two angles can easily be derived using the geometry shown in Fig. 2(a), as

$$\theta = 45 - \sin^{-1}\left(\frac{\cos \propto}{n_p}\right), \tag{2}$$

with n_p being the refractive index of prism. The SPR spectrum is characterized by the following parameters: resonant angle α_{SPR}, full width at half minimum (FWHM), and reflection minimum R_{min}. The two marked discontinuities before the SPR fall in Fig. 2(b) represent the critical angles for the materials the prisms are made up of (BK7 in the present case for both the prisms). The separation between the

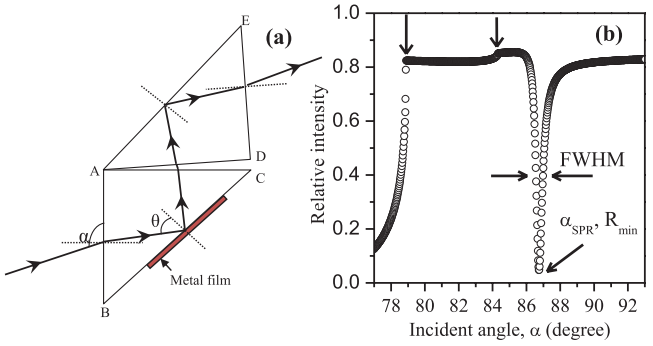

FIG. 2. SPR measurement with a two-prism setup. (a) Top view of prism table with ray diagram. (b) Typical SPR spectrum obtained with a two-prism setup.

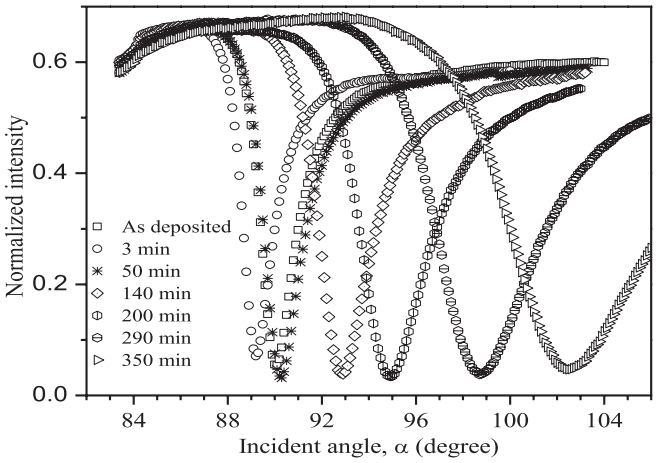

FIG. 3. SPR spectra of Al (6.3 nm)/Ag (38 nm) plasma oxidized for different durations.

critical angles represents the angle between the prisms. In fact, this knowledge of the angle between the prisms and intensity profile for bare prisms were used to ensure that the mechanical drift, if any, in the stepper motor used has no effect in the actual data obtained during SPR measurements. The intensity profile for bare prisms was reproduced, within 2% of variation in intensities, with both clockwise and anticlockwise rotations during standardization of the setup and before the starting of each batch of SPR measurement.

III. SPR MEASUREMENTS ON Al/Ag BI-LAYER

The outcome of the SPR measurements on Al/Ag bi-layer is presented in Fig. 3. The initial thicknesses of Al and Ag were 6.3 and 38 nm as noted from thickness monitor during thermal evaporation. The total time of plasma treatment was 7 h in a total of 33 steps of different durations. SPR spectrum was recorded after each step and only few SPR data of selected durations are given in Fig. 3 for convenient viewing. All the data, however, were analyzed in terms of α_{SPR} and FWHM. As observed from Fig. 3, both α_{SPR} and FWHM change in a particular manner (first decrease followed by increase) as the duration of plasma treatment increases. It is evident from the existence of SPR fall even after ~6 h of plasma treatment that unlike the saturation in natural oxidation of thin Al as observed by Yang *et al.*,[7] plasma oxidation is not saturated. The broadening and rightward shift in SPR fall indicates the formation of oxide layers of both Al and Ag during plasma treatment as the plasma was created in oxygen partial pressure. To confirm the formation of such oxide layers, glancing angle x-ray diffraction (GXRD) measurement was performed on the films before and after plasma oxidation. For this, additional films were grown on glass substrates simultaneously during the deposition of films over BK7 prism for SPR measurements. During plasma oxidation, the films on glass were also kept adjacent to prisms inside the chamber meant for SPR measurements. For comparison, bare Ag film on glass was also coated followed by plasma oxidation. The GXRD results for both Ag and Al/Ag films grown over glass are given in Fig. 4. Figure 4(a) shows the GXRD patterns for as deposited and plasma oxidized Ag film, whereas Fig. 4(b) shows the same for Al/Ag bi-layer. In both Figs. 4(a) and 4(b), the data for as deposited and plasma oxidized samples are given in bottom and top panels, respectively. The duration of plasma oxidation was 2 h for the films, of which the GXRD patterns are shown. The value of glancing angle for the data given here is 0.6° which was reached after optimizing for good intensity. The diffractions from different orientations are marked against the corresponding peaks in both the figures after matching the experimental data with JCPDS (Card Nos. 00-003-0796 and 01-087-0720 for Ag_2O and Ag, respectively). It can be noted here that no separate peak for metallic Al is observed in the lower panel of Fig. 4(b), which is as per expectation for the following reasons. First, a fraction of initial 6.3 nm thick Al gets converted into AlO_x by the time GXRD measurement is performed, thereby making the available Al thickness too thin to give appreciable peak. Second, the most intense peak for Al is from (111) orientation that appears at 38.23° (JCPDS Card No. 01-089-2837) which is very close to that for Ag. Thus, any peak due to 4-5 nm thick Al will be suppressed by the 38 nm thick Ag. As observed from Fig. 4(a), no peak corresponding to metallic Ag is found in plasma oxidized Ag film. However, Al covered Ag film shows Ag (111) even in the plasma treated sample as clear from the top panel of Fig. 4(b). This means

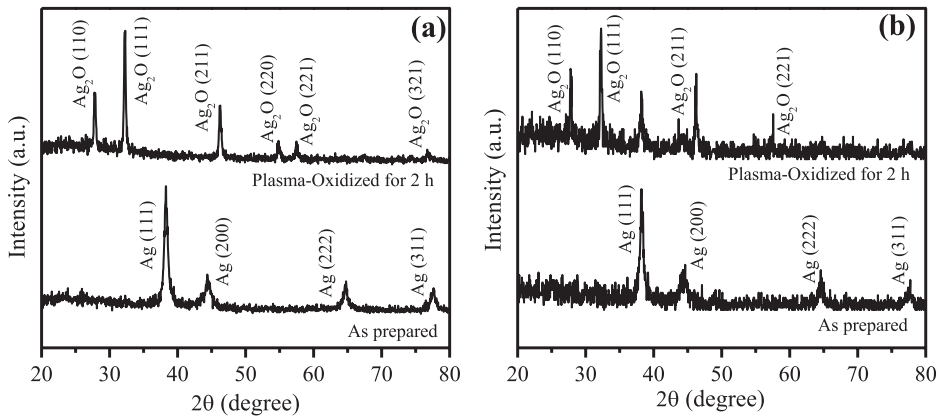

FIG. 4. GXRD patterns of (a) bare Ag and (b) Al/Ag both before and after plasma oxidation.

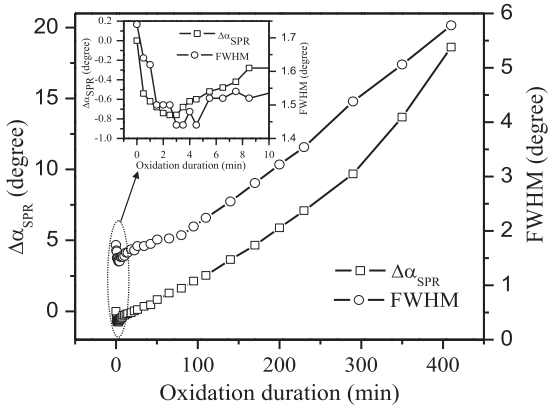

FIG. 5. Variations of shift in SPR minima and FWHM with oxidation duration. Inset: variations for initial 10 min.

that whole of Ag film in Al/Ag bi-layer is not converted into Ag_2O. Besides the surface oxide layer, rest of the initial Ag is in metallic state. Thus, comparison of Figs. 4(a) and 4(b) confirms that the oxidation of Ag film in Al/Ag is a controlled one whereas the same of bare Ag is uncontrolled. This conclusion asserts the SPR observations. Additionally, the top panel of Fig. 4(b) shows no separate peaks due to Al_2O_3, the most stable form of AlO_x. The possible reasons behind this could also be because of very small thickness of the oxide layer formed or the said layer could be amorphous. The first possibility was ruled out after performing GXRD measurements with varying glancing angle and observing no appreciable peak for Al_2O_3. Aluminum oxide has four allotropes including the amorphous Al_2O_3 that can form[13] at a temperature less than 50 °C. We conclude that the Al_2O_3 formed here with plasma oxidation is an amorphous one.

The changes in $\Delta\alpha_{SPR}$ and FWHM as a function of duration of plasma treatment were calculated from SPR data for all the steps of plasma treatment and presented in Fig. 5. As seen in Fig. 5, α_{SPR} shifts by a total of ~20° after plasma treatment for ~7 h giving rise to a value of 0.04° min^{-1} for $\Delta\alpha_{SPR}/\Delta t$. The important observation in the inset of Fig. 5 is that the values of $\Delta\alpha_{SPR}$ become negative as well as FWHM decreases for initial few minutes of plasma treatment. Here, the negative value of $\Delta\alpha_{SPR}$ indicates the leftward shift of SPR minima with plasma treatment as we define $\Delta\alpha_{SPR} = \alpha_{SPR}$ (after plasma treatment) $- \alpha_{SPR}$ (before plasma treatment). This particular observation is specific to the SPR measurements performed under low pressure as in present case and it cannot be observed in SPR studies done in atmospheric conditions. The reason behind this observation and the interpretation is as follows. After performing several simulations,[14] it was found that α_{SPR} and FWHM of SPR curves for pure metallic films will be lower compared to films containing non-metallic layers (usually oxides, sulfides, hydroxides, etc.) on the surface of the films. Hence, lowering of these two values indicate the cleaning of any non-metallic layers on the top of the film by converting them to metallic ones through plasma etching which is a common process in every plasma treatment. The maximum negative value of $\Delta\alpha_{SPR}$ and the duration for which $\Delta\alpha_{SPR}$ remains negative are different for different types and thicknesses of top layers on Ag. Thus, in the present case, the initial (for ~3 min) negative values of $\Delta\alpha_{SPR}$ and lower values of FWHM confirm the plasma etching of native oxide/hydroxide layers formed on Al layer. The value of $\Delta\alpha_{SPR}/\Delta t$ for initial 3 min during which maximum negative shift (0.78°) was observed is 0.26° min^{-1}. The increase in both $\Delta\alpha_{SPR}$ and FWHM afterwards indicates the oxidation of Al/Ag bi-layer.

IV. *IN SITU* MEASUREMENTS DURING PLASMA TREATMENT

In the usual SPR measurements where low pressure is not created or the sample under study is kept outside the vacuum chamber, the native oxide layers keep on forming. Although this layer can be cleaned when required by plasma etching, the cleaning/etching process cannot be detected/controlled. This is because the time required for native oxide layer formation is few ms for Al[13] whereas the same for completing SPR measurement is few minutes. On the other hand, when the SPR measurement is performed under low pressure, the method becomes an efficient way to monitor the plasma etching, which is already shown to be possible with the present setup. More importantly, *in situ* measurement of plasma cleaning/etching/oxidation can be performed with the setup. For this, normalized reflectivity can be measured as a function of time at different angular positions of probing points. Figure 6 shows one such typical intensity vs time plot.

The data presented in Fig. 6 were taken during 15 min of plasma treatment of a film that was initially Al/Ag bi-layer and was already plasma treated for 95 min before the above measurement. The probing point was 0.08° after the SPR minima of the SPR spectrum taken prior to this measurement. In order to interpret the *in situ* data, the important intensity values are labeled with dotted lines. These are the minimum characteristic changes observed during an *in situ* measurement with the exception that I_5 is not observed for plasma oxidation of short durations (less than 8 min). The conditions for intensity levels marked in Fig. 6 are as follows. (I_1) The value at which plasma was switched on, (I_2) the value immediately seen after switching on the plasma, (I_3) the value at which plasma was switched off, (I_4) the value immediately seen after switching the plasma off, and (I_5) the value shown after a

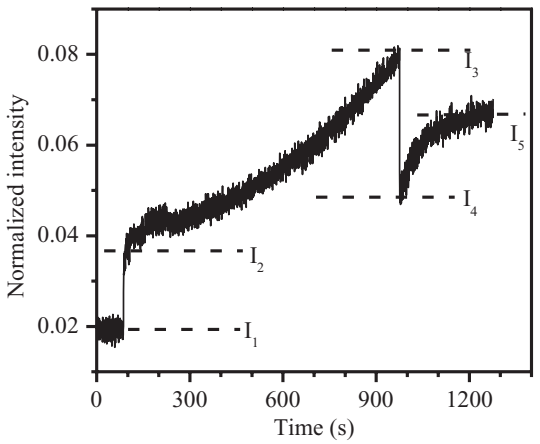

FIG. 6. *In situ* measurement during plasma treatment (see text for details).

sufficiently long time after switching the plasma off (with the level of low pressure maintained). As seen from Fig. 6, the actual change in intensity due to the effect of plasma on sample occurs between I_2 and I_3 whereas the magnitude of effective change in intensity due to plasma is I_5–I_1. The exponential increase of intensity between I_4 and I_5 is a temperature induced one. It shows the cooling of the film from a temperature raised by plasma heating. Thus, in addition to the oxidation dependent changes in thickness, n, and k of sample under study, the variation between I_2 and I_3 also includes the temperature dependent changes during heating. The typical variation between I_4 and I_5 for longer durations of plasma treatment can be made use of in determining the temperature dependency of reflectivity, R(T), of the multilayer structure as a whole. This, in turn, can indicate the temperature dependent dielectric functions of different layers. The difference I_3–I_4 gives the plasma intensity which should be same as I_2–I_1, provided no plasma etching occurs within the time between two data points are acquired (200 ms in the present case). This, however, was not found to be the case. All the three mathematical relations are possible between I_2–I_1 and I_3–I_4 depending upon the initial condition of sample, plasma power, probing point (angular position), etc. Both the value of change in intensity due to plasma etching and the duration of the same can be easily found from the plots similar to the one shown in Fig. 6. Thus, an intensity vs time plot similar to Fig. 6 is as informative during plasma treatment of thin films as any of the other measurements like sensorgram[3] obtained during bio-molecular interactions, the direct observations of chemical changes using surface plasmon spectroscopy,[15] and *in situ* differential ellipsometry measurements.[16] From the point of view of these *in situ* measurements during plasma treatment, the setup is first of its kind.

V. CONCLUSIONS

SPR measurements were performed on Al (6.3 nm)/Ag (38 nm) bi-layer, plasma treated for different durations at a pressure of 0.02 mbar. The SPR position was found to be shifted by ∼20° after a plasma treatment for ∼7 h. The shift was due to the formation of oxide layers during plasma oxidation. The formation of oxide layers was confirmed by GXRD. Combined analysis of GXRD and SPR data confirmed that plasma oxidation of Ag can be controlled. It was shown from *in situ* measurements that information about various processes like plasma etching, plasma oxidation, plasma heating, etc., can be obtained from different characteristic features of intensity vs time plot. Both the negative values of $\Delta\alpha_{SPR}$ and lower values of FWHM along with the *in situ* measurements confirm the plasma etching process. While top Al layer enables controlling plasma oxidation of Ag, the setup enables monitoring the same by SPR measurements. Thus, the setup designed is a first of its kind for the SPR based studies where creation of low pressure is a prerequisite, and particularly for the studies related to plasma-thin film interaction.

[1]H. Raether, in *Physics of Thin Films*, edited by G. Hass, M. H. Francombe, and R. W. Hoffmans (Academic, New York, 1977), Vol. 9, p. 145.
[2]E. Kretschmann, Z. Phys. **241**, 313 (1971).
[3]*Handbook of Surface Plasmon Resonance*, edited by R. B. M. Schasfoort and A. J. Tudos (The Royal Society of Chemistry, Cambridge, UK, 2008).
[4]V. S. Grinevich, L. N. Filevskaya, L. S. Maximenko, I. E. Matyash, O. N. Mischuk, S. P. Rudenko, B. K. Serdega, and V. A. Smyntyna, J. Nanomater. Mol. Nanotechnol. **2**, 1 (2013).
[5]K. K. Ostrikov, U. Cvelbar, and A. B. Murphy, J. Phys. D: Appl. Phys. **44**, 174001 (2011).
[6]A. K. Keshri and A. Agarwal, Nanosci. Nanotechnol. Lett. **4**, 228 (2012).
[7]J. Y. Yang, K. S. Yoon, J. H. Kim, W. J. Choi, J. H. Koo, C. O. Kim, and J. P. Hong, IEEE Trans. Magn. **41**, 2694 (2005).
[8]J. H. Park, K. S. Yoon, J. Y. Yang, E. K. Kim, C. H. Lee, C. O. Kim, and J. P. Hong, J. Appl. Phys. **92**, 3283 (2002).
[9]C. A. M. Knechten, Ph.D. thesis, Eindhoven University of Technology, Netherlands, 2005.
[10]B. C. Mohanty and S. Kasiviswanathan, Rev. Sci. Instrum. **76**, 033103 (2005).
[11]J. D. Cobine, *Gaseous Conductors* (Dover Publ., Inc., New York, 1968), pp. 114–115.
[12]F. Galvez, C. Monton, A. Serrano, I. Valmianski, J. de la Venta, I. K. Schuller, and M. A. Garcia, Rev. Sci. Instrum. **83**, 093102 (2012).
[13]C. Vargel, *Corrosion of Aluminium* (Elsevier, Oxford, UK, 2004).
[14]Simulations were performed with the winspall freeware code available for single prism followed by converting the data for two prism setup.
[15]C. Novo, A. M. Funston, and P. Mulvaney, Nat. Nanotechnol. **3**, 598 (2008).
[16]C. G. C. H. M. Fabrie, K. Knechten, J. T. Kohlhepp, H. J. M. Swagten, B. Koopmans, and W. J. M. de Jonge, Appl. Phys. Lett. **88**, 031909 (2006).